Journal of Applied Sciences and Nanotechnology

Journal homepage: jasn.uotechnology.edu.iq

Green Fuel Innovation: Enhancing Biodiesel Production with MCM-41 Mesoporous Silica Catalysis

[1]Hiba Kh. Ismaeel, [1]Talib M. Albayati[*], [2]Hayder A. Dhahad, [1]Farah T. Al-Sudani, [3]Issam K. Salih, [4]Sohrab M. Zendehboudi

[1]Department of Chemical Engineering, University of Technology- Iraq, 52 Alsinaa St., PO Box 35010, Baghdad, Iraq
[2]Mechanical Engineering Department, University of Technology- Iraq, 52 Alsinaa St., P.O. Box 18310, Baghdad, Iraq
[3]Department of Chemical Engineering and Petroleum Industries, Al-Mustaqbal University, Babylon 51001, Iraq
[4]Department of Process Engineering, Memorial University, St. John's, NL A1B 3X5, Canada

A R T I C L E I N F O

Article history:
Received: May, 24, 2024
Accepted: August, 13, 2024
Available online: September, 10, 2024

Keywords:
Nano-catalytic transesterification,
Homogenous catalyst,
Green energy applications,
Reaction kinetics,
Mesoporous silica NPs

Corresponding Author:
Talib M. Albayati
Talib.M.Naieff@uotechnology.edu.iq

A B S T R A C T

In this study, mesoporous silica nanoparticles (MSNs) with a hexagonal structure and large surface area were synthesized via a sol-gel method. The properties of the synthesized MCM-41 catalyst were characterized using BET, EDX, XRD, and FTIR analyses. The results showed that the MCM-41 had a high surface area of 966 m2/g and large pore volume of about 0.91 cm3/g. Sunflower oil was converted to biodiesel in a batch reactor at different temperatures (40, 50, 60 °C), methanol-to-oil molar ratios (6:1, 9:1, 12:1), catalyst loadings (0.7, 0.9, 1.25 wt%), and reaction times (up to 80 min) using the prepared catalyst under atmospheric pressure. The biodiesel yield was found to reduce when the reaction time exceeded 1 hour despite maintaining the catalyst. The maximum biodiesel yield of 45% was obtained under optimal conditions of a 9:1 methanol-to-oil ratio, 1.25 wt% catalyst loading, 60 °C temperature, and 60 min reaction time. GC-MS analysis characterized the biodiesel composition and properties. The synthesized biodiesel showed improved properties compared to conventional fuels, with linoleic acid methyl ester (C17H34O2, 25.93%) as the main component. The MCM-41 catalyst exhibited remarkable catalytic activity and could be recovered, regenerated, and reused, reducing reaction costs. This makes it a potential alternative to homogeneous catalysts that complicate product separation.

https://doi.org/10.53293/jasn.2024.7423.1294, Department of Applied Sciences, University of Technology - Iraq.

1. Introduction

Crude oil is the most essential energy source worldwide. The economic growth of most countries depends on the energy supply. Worldwide energy consumption is predicted to rise by 33% by 2035 due to the rapid spread of industrialization and urbanization [1]. However, because to the exhaustion of non-renewable forms of energy and their detrimental effects on the ecosystem, such warming of the planet, it is necessary to search for sustainable, energy-efficient, and conservation methods [1]. Global attention has been directed to more eco-friendly and sustainable techniques for generating renewable energy sources [2]. Renewable energy provides non-toxic,

biodegradable supplements that offer cleaner, more environmentally friendly approaches to overcoming economic and environmental challenges [3]. "Biofuel" is one of the oldest and most extensively utilized renewable energy sources. Biodiesel is a type of biofuel that is biodegradable, non-toxic, and renewable energy source. Various substrate sources, including algae, animal fats, oilseeds, and vegetables, are suitable for manufacturing biodiesel. The raw material selection procedure considerably influences the viability and economics of biodiesel manufacturing; hence, it is critical since using expensive substrate might make the manufacture of biodiesel unprofitable [4]. Among various types of vegetable oil, sunflower oil represents an excellent potential substrate for biodiesel use due to its comparable properties to Petro diesel; the primary parameters for assessing biofuel's energy content and combustion characteristics are calorific value and cetane number. Several studies investigated the possibilities of cultivating sunflower seeds for biodiesel production. The results were beneficial, with a high biodiesel yield compared to numerous oils [5].

The variety of techniques for producing biodiesel urges exploring new and ideal procedures combined with the highest yield. However, no process is flawless, as every strategy has its drawbacks. Many investigations have been done to reduce the methods that use catalysts, which include leaching, deactivation, and separating from the product of the reaction since they are essential for increasing the effectiveness of transesterification reactions.

For biodiesel manufacturing, heterogeneous catalysts often have fewer challenges than homogeneous catalysts. However, issues still need to be resolved, including long processing periods, slow reaction rates, and product purification and separation difficulties. Nano-catalytic transesterification can successfully address the abovementioned limitations because of its larger surface area and higher catalytic activity than conventional catalysts; transesterification-related nanocatalysts exhibited various benefits for biodiesel production. They also show excellent stability, strong surface area-to-volume proportion, saponification procedure resistance, and a sizable reuse ability factor. Many scientists are investing a lot of work into designing new nanocatalysts and improving their properties for better catalytic performance that is more effective and efficient [6]. Several investigations on different nano catalyst-catalyzed transesterification processes employing various biodiesel substrate materials are provided in **Table 1**.

Mesoporous catalysts are nanocatalyst forms that have garnered much attention in biodiesel production studies due to their unique characteristics. These characteristics make it easier for the reactants to go from the acidic sites of the catalyst to the active sites inside its internal structure. Several mesoporous nanomaterials have recently been developed. The International Union of Pure and Applied Chemistry (IUPAC) has divided mesoporous nanomaterials into ordered and non-ordered categories [28]. In particular, Due to their remarkable features—such as identical pore-size distribution, enormous surface area, crucial volume of pore, accessible walls substance, suitable for mass transfer characteristics, and extraordinary thermal and mechanically stable—ordered mesoporous silicate and ordered mesoporous carbon have attracted a lot of research attention [29,30]. Mesoporous silica nanoparticles are distinguished as superior heterogeneous catalyst substrates. MCM-41 is a common mesoporous silica material discovered and characterized by its uniform size of the pore, substantial pore volume, and well-organized mesoporous shape that takes on a hexagonal symmetry [31,32]. Siloxane groups are distributed throughout the bulk of these materials, whereas silanol groups are located on the exterior surface [33].

In this study, MCM-41 catalysts produced from Tetraethyl Orthosilicate, a source of silica, were utilized to manufacture biodiesel from sunflower oil via the sol-gel process. This mesoporous catalyst was selected because of its appropriate size of pore for the proposed reaction. Employing a solid catalyst facilitates the separation of the product as soon as being formed from the reaction medium. Recovering the catalyst allows for potential reactivation and reuse, lowering the total cost of the industrial process. The objective of this research is to examine the operational parameters, such as loading of the catalyst, reaction temperatures, reaction durations, as well as the molar ratio of methanol/ sunflower oil.

Table 1: nanocatalysts utilized for biodiesel synthesis.

catalyst	feedstock	Reaction conditions:- (Methanol to oil molar ratio) (Catalyst amount (%W)) (Reaction temperature (^{O}C)) (Time (min))	Yield%	Ref.
Nano-$Ca(OCH_3)_2$	Microalgae oil	30:1, 3, 80, 180	99	[7]
$MgO/MgFe_2O_4$	Sunflower oil	12: 1, 4, 110, 240	91.2	[8]
$CaO/CuFe_2O_4$	Chicken oil	15: 1, 3, 70, 240	94.52	[9]
MgO	Goat fat	12: 1, 1, 70, 180	93.12	[10]
CaO	Waste cooking oil	8: 1, 1, 50, 90	96	[11]
Waste-based CaO	Microalgae oil	11: 1, 2, 60, 180	92	[12]
Li/Fe_3O_4	rapeseed oil	12: 1, 0.8, 35, 30	99.8	[13]
Li-TiO2/Feldspar	karanja	10:1,2, 50, 120	96.4	[14]
Li-TiO2/Feldspar	Saflower oil	5:1, 2, 50, 120	96.5	[14]
Li-TiO2/Feldspar	castor oil	15:1, 2, 60, 120	96.1	[14]
CaO	Soya-bean oil	15:1, 8, 65, 120	80	[15]
ZrO_2-TiO_2@MGO	used cooking oil	3:1, 4.7, 65, 180	99	[16]
CdO_2	Malabar Ebony seed oil	1:9, 0.5,90,180	94	[17]
ZIF-8 MOF	soybean oil	20:1, 7, 90,150	97.4	[18]
$NixZn_{1-x}$ Fe_2O_4	neem seed oil	16.5:1, 3, 70, 50	93	[19]
CaO	soybean oil	20:1, 8, 65, 150	81.3	[20]
CuO	Citrullus colocynth Seed Oil	8:1, 0.365, 85, 120	95	[21]
Fe_3O_4/SiO_2@ZnO	Waste-cooking-oil	9:1, 2, 60, 30	88.3	[22]
CeO_2	Descurainia sophia L	8:1, 0.3, 90,210	98	[23]
$NiFe_2O_4$	Acacia furnesiana seed oil	14:1, 4.61, 65, 53	93.1	[24]
CaO/Fe_2O_3	waste cooking oil	11:1,1,60,70	90.4	[25]
MGO@TiO_2Ag	waste cooking oil	2.52:1, 4.15, 60, 169	96	[26]
GO@ZrO_2–SrO	Waste cooking oil	4:1,1,120, 90	91	[27]

2. Experimental Work

2.1 Materials

Hubei Bluesky New Material Inc., Xiantao, China, supplied TEOS, Si $(OC_2H_5)_4$ (tetraethyl orthosilicate) with a purity level of 98%, while Interchiniques SA, France, supplied cetyltrimethylammonium bromide (CTAB, $C_{19}H_{42}BrN$) with a purity level of 98%. Simultaneously, 99% pure granular sodium hydroxide (NaOH) was provided by CHEM-LAB (Belgium). An Iraqi producer provided deionized water with zero conductivity and seven pH. Additional raw ingredients from Sigma Aldrich were obtained for this work, involving methanol with an analytical purity of 99.5% and a Pellet of potassium hydroxide (96.0%). The sunflower oil was purchased from a local market. Phenolphthalein was used as an indicator. The sample's acidity and FFA (free fatty acid) content were determined using titration. The mixture was gradually mixed with a few drops of KOH (potassium hydroxide) solution and methanol until the colour changed into purple. Before biodiesel was generated, GC-MS determined the complete chemical composition of sunflower oil. **Table 2** shows the primary components and fatty acid makeup of oil. Sunflower oil's fatty acid composition values are consistent with those reported in previous scholarly publications [34,35].

Table 2: Fatty acid composition of sunflower oil.

No.	Resident Time (min)	Area (%)	Name of component	Chemical Formula	Free Fatty acid	Molecular wt.
1	20.171	13.92	(methyl palmitate)	$C_{17}H_{34}O_2$	C17:0	270
2	22.733	68.88	9,12Octadecadienoic acid (Z, Z)- (linoleate acid)	$C_{19}H_{34}O_2$	C19:2	294.5
3	23.027	7.75	Methyl stearate	$C_{19}H_{38}O_2$	C19:0	298.5
4	23.217	1.85	9,12Octadecadienoic acid (Z, Z)- (linoleate acid)	$C_{19}H_{34}O2$	C19:2	294.5
5	23.693	0.22	9,12Octadecadienoic acid (Z, Z)- (linoleate acid)	$C_{19}H_{34}O2$	C19:2	294.5
	others	2.38				

2.2 The MCM-41 preparation

The sol-gel technique was utilized to create (Mesoporous Silica Mobil Composition of Matter) No. 41 (MCM-41), with (TEOS) as a silica source and (CTAB) as a guiding agent for structure [36]. Initially, (0.34 grams) of NaOH and (30 millilitres) of deionized water were used to dissolve 1 g of CTAB. After stirring the mixture for approximately 1 hour at room temperature, the remaining 5.78 grams of TEOS was gradually added. Homogenous-mixture output was continuously hydrothermally heated to 110 °C for 96 hours in an autoclave. The filtered solid product was washed with deionized water to remove partial surfactants. The resultant solid was dried overnight at forty degrees Celsius [37]. As seen in **Fig. 1**, the product was calcined at (550°C) for six hours to remove the surfactant and produce a white catalyst powder.

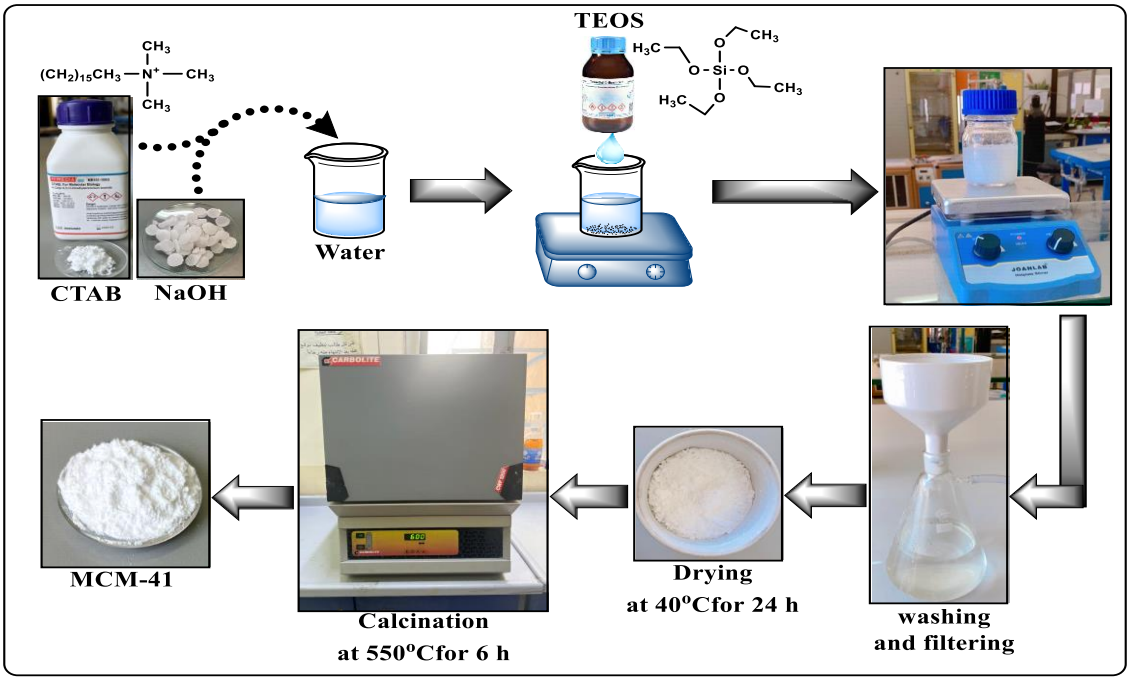

Figure 1: The synthesis steps for MCM-41which prepared at 110 °C and atmospheric pressure for 96 hours.

2.3 Catalyst reusability

Centrifugation separated the mixture obtained from the last step of the initial transesterification process from the consumed catalyst. Then, the final product is transferred to be purified. The utilized catalyst was restored via an hour-long cyclohexane wash, stirring at 100°C, and a drying phase at 120°C. Following the drying stage, the procedure continues with a one-hour calcination at 500°C. The catalyst is renewed and prepared for reuse [38].

3. A trans-esterification Process

In the transesterification process of sunflower oil, MCM-41 catalyst is used. The temperature was adjusted between 40 and 60 °C by a temperature controller, and a speed controller comprised the experimental reactor setup, which consisted of a (250 millilitres) three-neck flat bottom glass flask with a mechanical stirring (MS) hot plate. The thermometer for measuring the reaction's temperature is placed in a tight rubber stopper on one side of the reactor's necks. Another side of the neck was used to extract the specimen of oil with an alcohol catalyst mixture. A condenser has been added to the reactor to facilitate methanol recovery, having a boiling temperature of (64 °C) and tending to evaporate at increased temperatures during reactions. It also assists in maintaining the reactor's internal atmospheric pressure. The reactor was set on the hot plate, and the required amount of vegetable oil was added. After a specific volume of catalyst-mixed methanol liquor was added to the reactor, then turned on the mechanical stirrer to create a stirring action at 800 rpm, which started the reaction. As shown in **Fig. 2**, the reaction of the trans-esterification was conducted in a laboratory-scale reactor using a batch reactor.

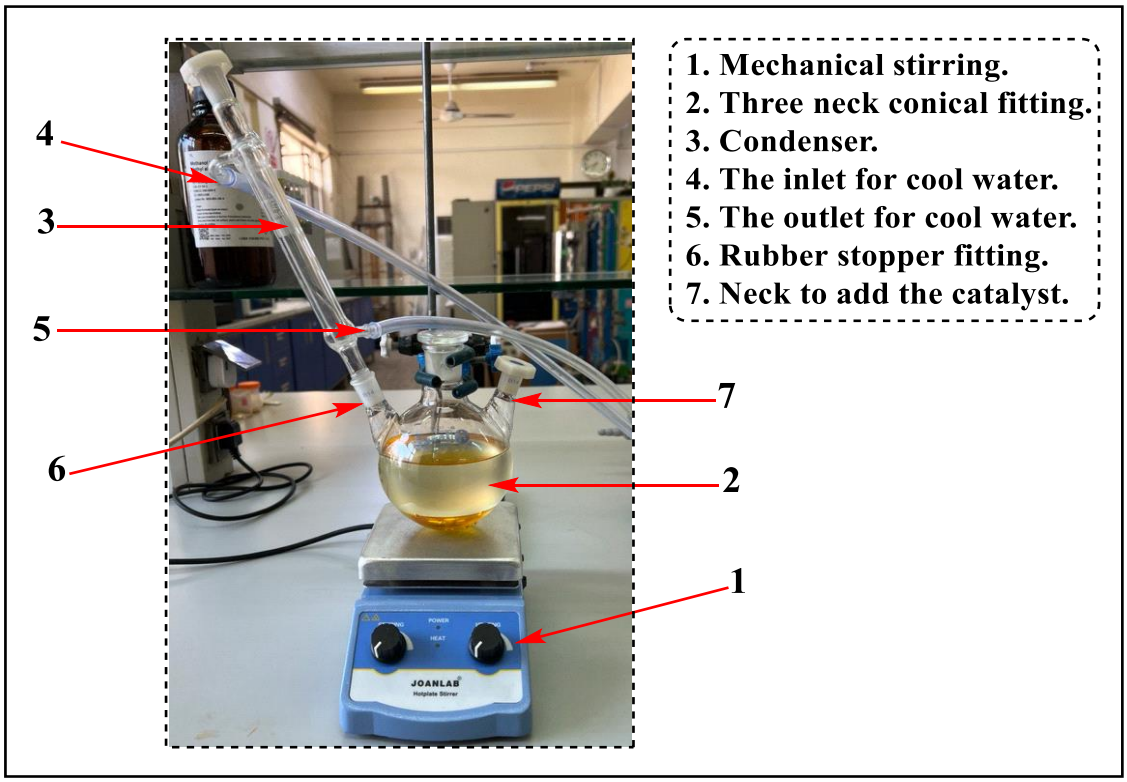

Figure 2: Experimental setup.

The yield of the trans-esterification reaction was calculated by the following Equation:

$$Yield\ \% = \frac{Production\ FAME}{Initial\ weight\ of\ oil} \quad (1)$$

4. Catalyst Characterisation

The X-ray diffraction (XRD) pattern of the synthesised MCM-41 material is shown in **Fig. 3**. This pattern exhibited a distinct peak at a 2θ angle ranging from 2.0° to 2.2°, indicating microporosity and a regular, well-organised, two-dimensional, hexagonal structure with long-range ordering within the channels [39-41]. Also, the XRD pattern exhibited two minor peaks at 2θ angles ranging from 3.8°-3.6° and 5.8°-5.2°, which can be attributed to the (d100, d110, and d200) crystallographic planes of the p6 mm lattice structure of MCM-41 material [39,41].

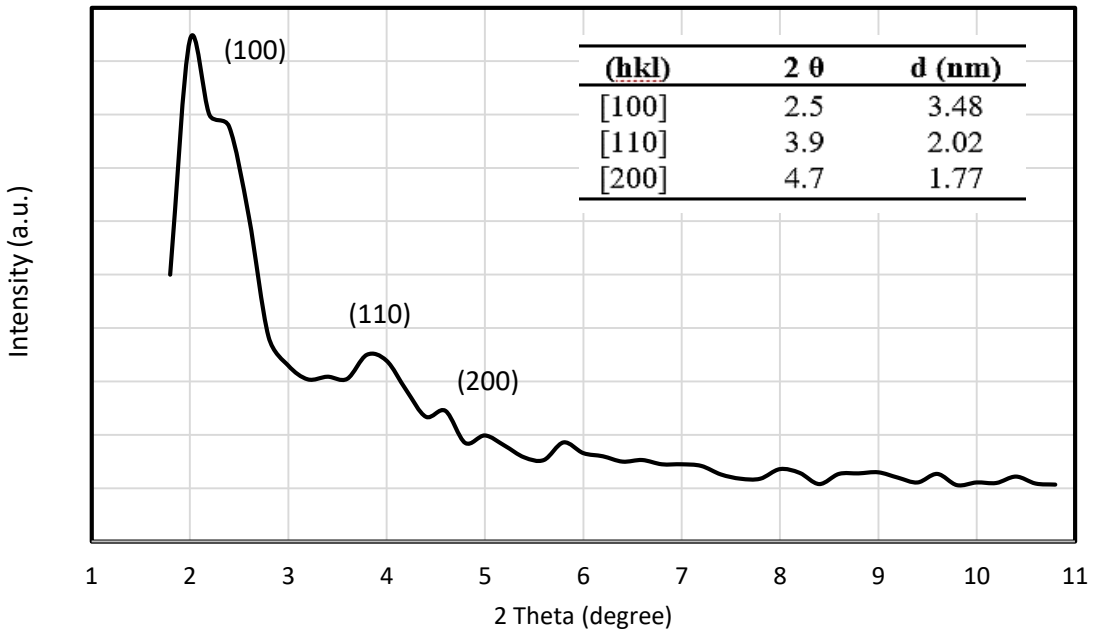

Figure 3: X-ray diffraction patterns of MCM-41.

Table 3 documented the findings from measuring the Brunauer–Emmett–Teller surface area, volume of pore, and pore size of MCM-41 mesoporous additives. The MCM-41 material has a significantly huge surface area of (966 m2/g). Utilising the CTAB cationic surfactant as an activating agent facilitates the generation of additional pores and the enlargement of pre-existing pores. The MCM-41 material exhibits a large pore volume of 0.91 cm^3/g.

Table 3: Surface properties of pure MCM-41.

Adsorbent	Specific area of surface (BET) (m^2/g)	Volume (cm^3/g)	Size of Pore (nm)
MCM-41	996	0.91	3.0

The morphology of the mesoporous MCM-41 is investigated using Energy Dispersive X-ray Spectroscopy-Scanning Electron Microscopy (EDX-SEM). The SEM image reveals that pure MCM-41 comprises smooth-surfaced agglomeration spherical particles, as shown in Fig. 4a. These findings agree with the results obtained from the previous work of Costa et al. [42]. The elemental composition of the MCM-41 is examined using EDX fundamental analysis. The EDX graph shows that MCM-41 mainly consists of O, Si, and C—the wt% and atomic% (Fig. 4b). The atomic ratio between O and Si is about 2:1. To acquire accurate wt% values for the compounds, EDX graphs are created at various spots on the SEM images. No traces of other elements were found in the loaded or modified samples because EDX is unreliable when only minimal elements are detected. Resulting from the area over which EDX is performed might not be large enough to identify the presence of certain components. In addition to the unequal distribution of components, EDX may be ineffective.

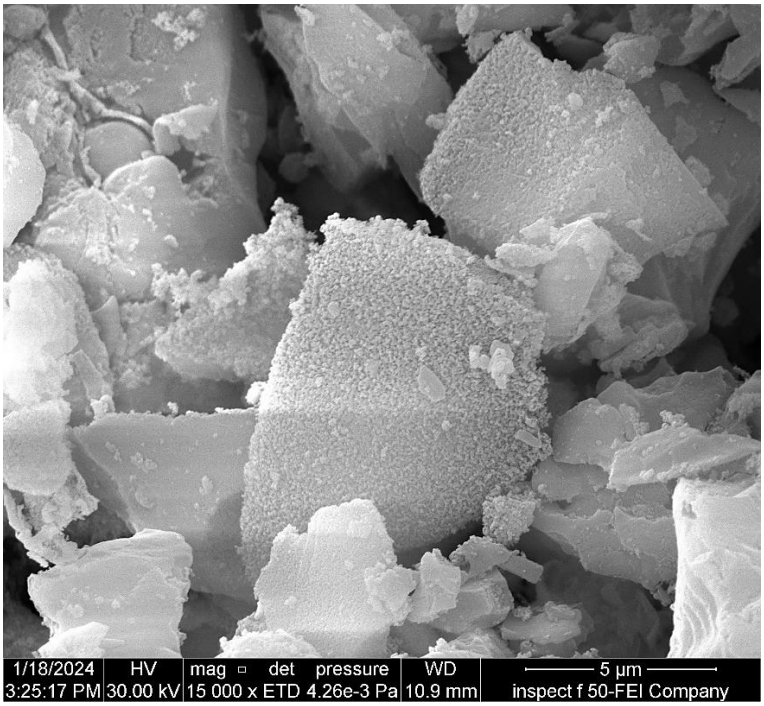

(a)

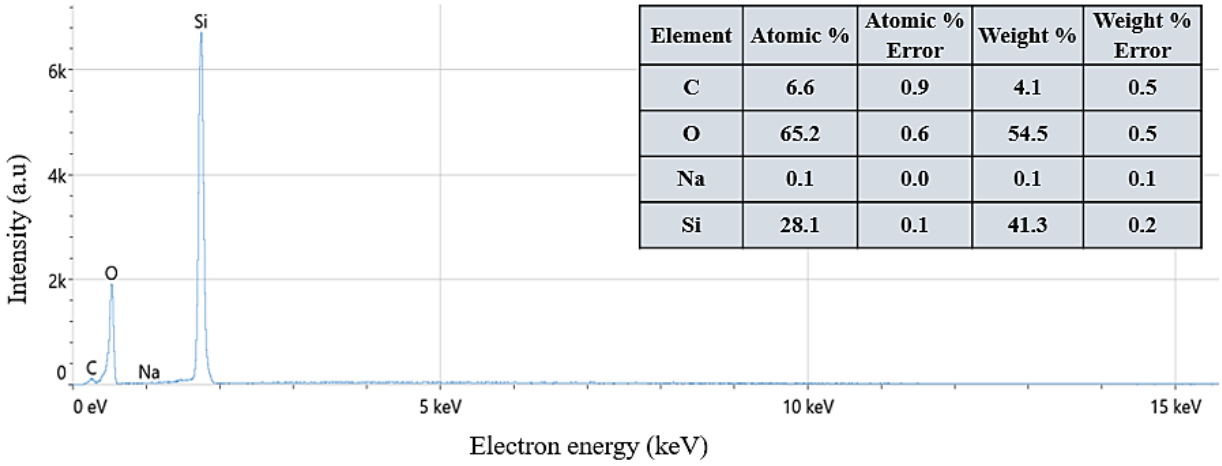

Element	Atomic %	Atomic % Error	Weight %	Weight % Error
C	6.6	0.9	4.1	0.5
O	65.2	0.6	54.5	0.5
Na	0.1	0.0	0.1	0.1
Si	28.1	0.1	41.3	0.2

(b)

Figure 4: a) illustrates SEM image at 15,000 magnification and **b**) EDX analysis of elements for MCM-41which prepared at 110 °C and atmospheric pressure for 96 hours.

A Fourier-transform infrared (FTIR) spectrometer is employed to determine the functional group on the surface of produced MCM-41. **Fig. 5** illustrates the infrared spectra obtained for MCM-41. The observed bands at 424.34, 447.49, 443.63, 806.25, 869.41, 1072.42, and 1087.85 cm-1 could be attributed to symmetric as well as asymmetric stretching vibrations of the Si–O–Si bonds. These vibrations indicate the formation of a condensed mesoporous silica system [43-45]. The band at (968.27 cm-1) is related to the (Si–O) stretching vibration of (Si-OH) within the MCM-41 framework. The existence of adsorbed molecules of water is responsible for the appearance of the 1647 cm-1 band, which can be related to the bending vibration of these molecules. A significant level of absorption is noticed at a wavenumber of (3614.60 cm-1) which is attributed to the presence of unbound (Si-OH). Also, the

band at (3595.31 cm-1) is determined to originate from (hydrogen-bonded) Si-OH groups to physically adsorbed H_2O molecules [43,45]. The types of bands are displayed in **Table 4**.

Table 4: Summarized the functional groups on the surface of produced MCM-41 with the type of their bands.

Absorption (cm^{-1})	Group	Appearance
3614	Si-OH stretching	Medium, sharp
1512	O–H stretching	strong
1072	Si–O–Si stretching	Strong, broad
964	Si–O bending	strong
806	C-C bending	Medium

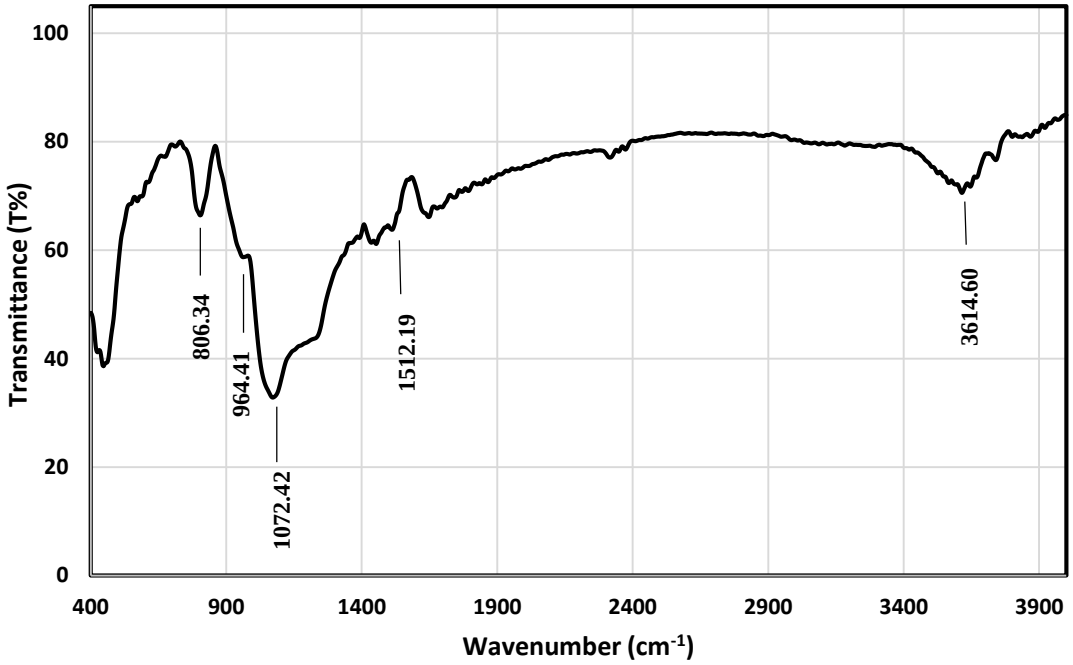

Figure 5: The infrared spectra obtained for MCM-41which prepared at 110 °C and atmospheric pressure for 96 hours.

5. Effect of Reaction Conditions on Biodiesel Produced

Various factors influence the study of the reaction conditions trans-esterification reaction for sunflower oil with alcohol (methanol) in a batch reactor with the heterogeneous prepared MCM-41 Nano catalyst were investigated, such as time of reaction, temperature of the reaction, catalyst loading, and molar ratio of (methanol to sunflower oil). The prepared catalyst activity was compared under optimised conditions derived from experimental results. Subsequently, the stability of the prepared catalyst was assessed through catalyst reuse in transesterification reactions.

5.1 Effect of Reaction Time

The time of reaction and the catalyst type have an impact on the time-dependent fluctuations in biodiesel yield, although the molar ratio of (methanol/ oil) remains constant. Fig. 6 represents the trends of the reaction time effect. For instance, with an MCM-41 to sunflower oil ratio of 1.25 wt% and a Methanol: Oil molar ratio of 9:1, the reaction temperatures at (40, 50, and 60 °C) were investigated in a batch reactor. The biodiesel yield progressively increases throughout the reaction duration until reaching peak conversion within 60 minutes at a reaction temperature of (60 °C). This observation suggests that at a particular time and temperature, the catalyst and conditions of reaction used in an experiment are favourable for converting sunflower seed oil into biodiesel.

5.2 Effect of Reaction Temperature

Reaction rates are temperature-dependent functions by Arrhenius's equation. Hence, the temperature of the reaction plays a vital function in the kinetics of reactions. Because methanol and sunflower oil transesterify in the liquid phase, the temperature of the reaction should not exceed methanol's boiling point of (64°C) at atmospheric pressure. The biodiesel yield with time at various temperatures is displayed in **Fig. 6** Using constant amounts of both methanol/oil molar ratios equal to (9:1) and 1.25wt% MCM-41 catalyst regarding sunflower oil at 40, 50, and 60 °C at times ranging from 10 to 80 minutes. The initial conditions in the batch reactor were selected based on recommendations from many researchers cited in a literature review [46,47].

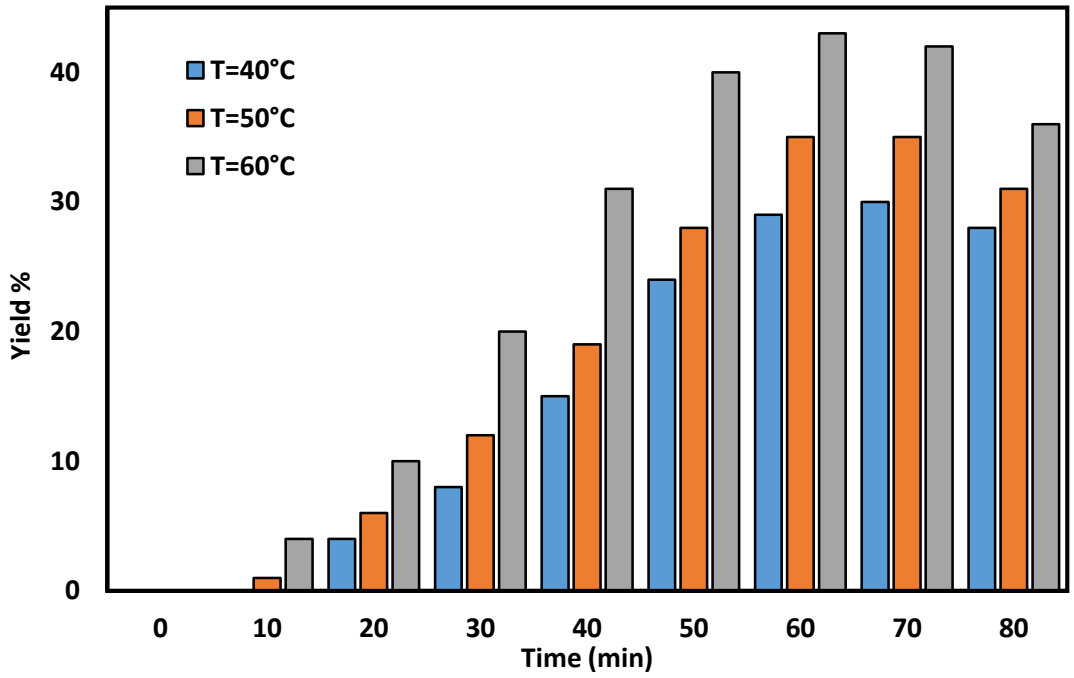

Figure 6: Effects of reaction temperature on yield of biodiesel using1.25 wt% of MCM-41 concerning sunflower oil, 9:1 methanol to sunflower oil Molar Ratio at different times.

As depicted in **Fig. 6**, a significant correlation between biodiesel yield, and temperature, demonstrating an increase with higher temperatures. For instance, at 40°C, the biodiesel yield reaches approximately 25% after 50 minutes, while at 60°C, the yield rises to about 40% within the same timeframe. This observed trend is consistent with predictions, as increasing temperatures enhance molecular activity, providing more energy for molecules to overcome reaction barriers and facilitate reactions following the collision theory [48].

Another contributing factor is decreased reactant viscosity with rising temperatures, promoting enhanced molecule diffusion through catalyst pores. **Fig. 6** illustrates that, within the initial 60 minutes across the different temperatures, the reaction predominantly occurs at the catalyst's active sites. Subsequently, the yield increased until approximately 70 minutes, after which biodiesel yield diminished due to MCM-41 deactivation. This

deactivation is attributed to water molecule clustering within the catalyst pores, influenced by the hydrophilic nature of MCM, intensifying the reverse reaction and reducing conversion [47,49]. The peak yield at 60°C is attained after 60 minutes, indicative of reaching equilibrium quickly, while the maximum yield at 40°C is achieved after 70 minutes. This discrepancy can be explained by the rapid reaction at 60°C causing early catalyst deactivation, whereas the slower reaction at 40°C delays catalyst deactivation.

5.3 Effect of methanol/Oil Molar Ratio

The transesterification process of sunflower seed oil with alcohol (methanol) is a reverse process that occurs at a molar ratio of 3:1 between the two substances. Since the reaction is reversible, an excess amount of alcohol (methanol) is used to shift the reaction's equilibrium in the direction of product formation. As shown in **Fig. 7**, three methanol/oil molar ratios6:1, 9:1, and 12:1, were employed in transesterification reactions with a constant concentration of 1.25 weight per cent catalyst at (60°C) for different times (10 to 80 min) in a batch reactor.

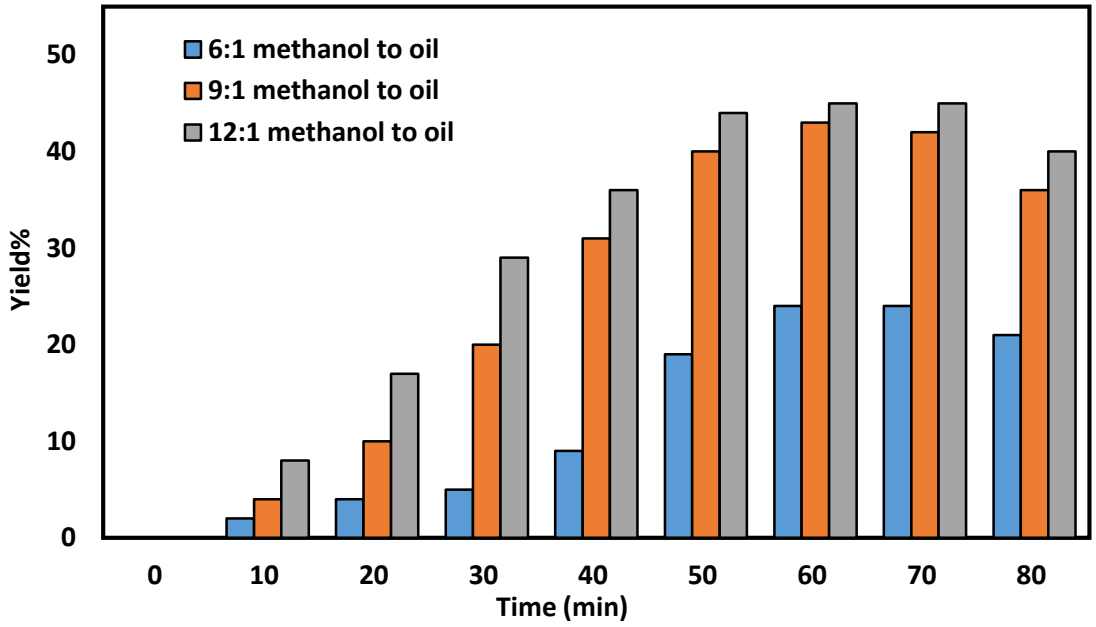

Figure 7: Effects of methanol on sunflower oil Molar Ratio on yield of biodiesel using 1.25 wt% of MCM-41 concerning sunflower oil and (60°C) of temperature at different times.

Fig. 7 illustrates a notable enhancement in biodiesel yield as the molar ratio of methanol to sunflower oil increases from (6:1 to 12:1). Specifically, after 60 minutes, the yield shows a substantial rise from 24% at a 6:1 ratio to 45% at a 12:1 ratio. However, a further increase in the molar ratio (from 9:1 to 12:1) did not significantly improve. Therefore, the optimal ratio for this parameter appears to be 9:1 methanol to sunflower oil. This finding aligns with various studies by Kumar et al. [50], Yin et al. [51], Mohod et al. [52], and Mohan et al. [53]. Determining the reactive medium's viscosity is another factor affecting the transesterification reaction. a mixture of methanol and oil becomes less viscous as the methanol-to-oil ratio rises because methanol has a lower viscosity than sunflower oil. As a result, at low methanol-to-oil ratios or high viscosities, a diffusion process was seen as a limiting process toward MCM-41 particles in the mixture [54].

5.4 Effect of catalyst dose

Sunflower oil was transesterified with methanol using various weight percentages of the MCM-41 catalyst to evaluate the catalyst's activity. Reactions were carried out with a constant methanol/ oil molar ratio (9:1) and at a constant temperature of (60°C). The effects of various weight percent ratios of MCM-41 to oil of 0.7%, 0.9%, and 1.25% wt% on the transesterification reaction are shown in **Fig. 8**. The transesterification process of sunflower oil shows a direct correlation to the percentage of catalyst loading MCM-41. This correlation is anticipated as a higher

catalyst amount provides a huge surface area as well as more active sites for the transesterification reaction to occur. Consequently, the maximum yield is achieved when the maximum amount of catalyst is loaded, i.e., at 1.25% loading, resulting in a yield of approximately 43% after 60 minutes.

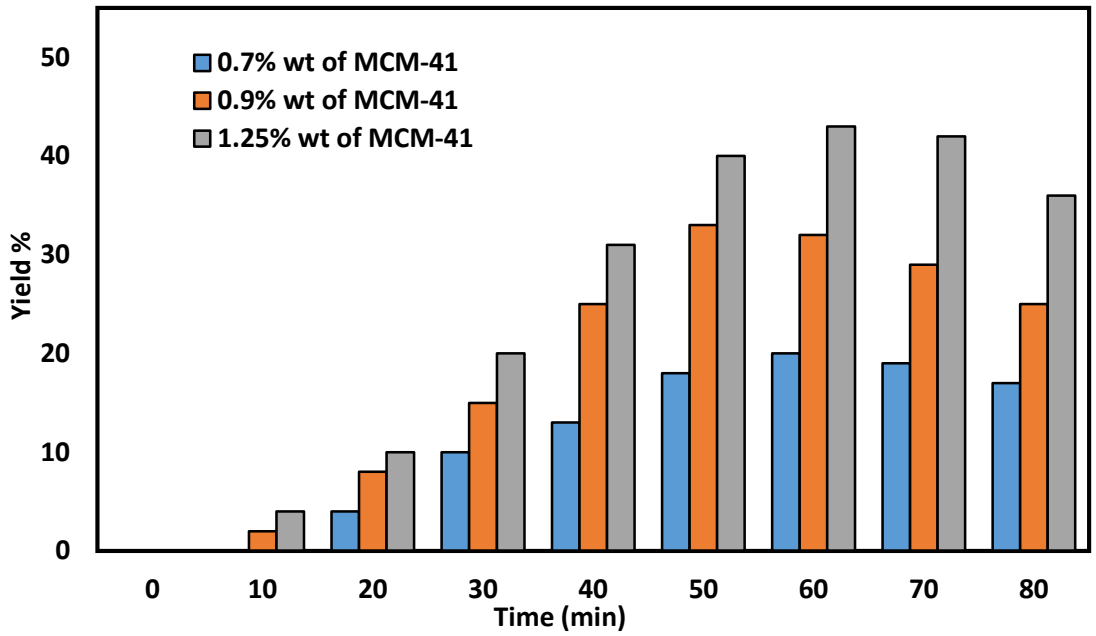

Figure 8: Effects of catalyst dose on yield of biodiesel using 9:1 methanol to sunflower oil Molar Ratio and (60°C) of temperature at different times.

In heterogeneous transesterification, an increase in catalyst loading boosts the number of particles for the catalyst as well as active sites, improving triglycerides' (TG) and alcohols' accessibility to the catalyst's surface. However, because there is less interstitial space between triglycerides (TG) and (alcohol molecules) when the catalyst loading is exceeded, biodiesel conversion or yield may be negatively or hardly affected [55]. An excess catalyst beyond the optimum value can also form an emulsion layer, complicating biodiesel separation [56]. The impact of catalyst concentration on the yield of reaction indicates that loading excessive catalyst amounts can lead to soap formation, limiting the conversion of (TG) to esters [57]. Consequently, insufficient catalyst loading can result in unsatisfactory biodiesel yield and higher production costs. Thus, determining the ideal amount of catalyst is essential for effectively converting triglycerides into fatty acid methyl esters (FAME) [58].

6. Effect of Catalyst Reusability on Biodiesel Yield

The ability to recycle heterogeneous catalysts is a major benefit compared to homogeneous ones. The synthesized MCM-41's reusability was assessed under ideal circumstances, which included (60°C), a (9:1) methanol/ oil molar-ratio, and 1.25wt% of MCM-41 for a single transesterification cycle. The solid catalyst was filtered to separate from the reaction mixture after the transesterification reaction. The techniques used for recovering the wasted catalyst from the reaction products were filtration and regeneration. The catalyst undergoes regeneration by washing with cyclohexane for 1 hour, stirring at (100°C), followed by a drying step at (120 °C). Post-regeneration, the catalyst is then reactivated and will be ready for reuse [38]. The regenerated solid catalyst was combined with precise quantities of fresh sunflower oil and methanol, identical to those used in the initial cycle, for additional recycling. The results of the recycling tests conducted on the reused catalyst over 80 minutes are shown in **Fig. 9**.

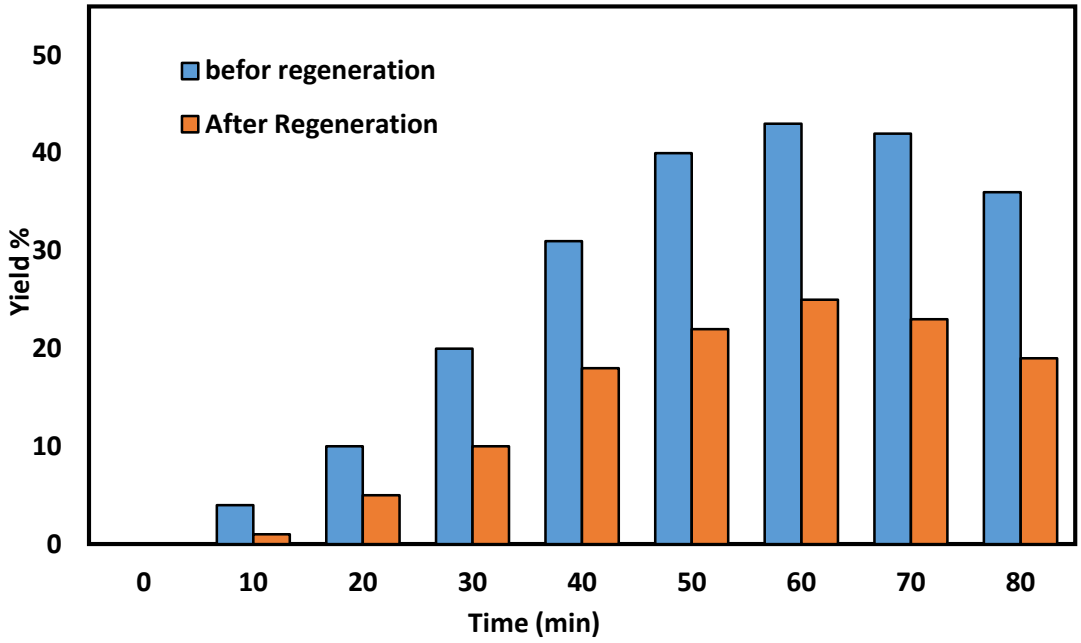

Figure 9: Regeneration catalytic behavior for 10%Ba/20%KOH@MCM-41 regenerated catalysts yield of biodiesel using 9:1 methanol to sunflower oil Molar Ratio, and 1.25 wt% of a catalyst for sunflower oil at 60°C of reaction temperature.

After regenerating the catalyst, biodiesel fuel production decreased compared to the production levels before regeneration. After regeneration, the maximum biodiesel yield was (25% after 60 minutes) and decreased as the reaction time increased. Reusing the catalyst after activation in transesterification processes for sunflower oil to produce biodiesel multiple times presents significant economic benefits by reducing the cost of employing completely novel and expensive catalysts. It can be inferred that extended reaction times hurt these sites' activity, occasionally producing an increase in glycerol formation by lowering the expenses associated with using entirely new and costly catalysts.

7. Testing Components and Properties of Biodiesel

7.1 GC-MS Chromatogram Analysis

Chromatography analysis is a versatile tool that can be used to identify a specific substance in biodiesel samples, including pollutants as well as methyl esters of fatty acids. In recent biodiesel quality control analysis, GC-MS is essential. As a result, it has broad applicability in the analysis of biodiesel composition [59]. In Biodiesel Testing Instrument Conditions; Analytical Column: Agilent HP-5ms Ultra Lite (30 m length x 250 μm inner diameter x 0.25 μm film thickness) Gas Chromatograph: Agilent (7820A) USA GC Mass Spectrometer Volume of injection (1) μl GC pressure of 11.933 psi Line of Inlet Aux heater temperature: (250 °C); carrier temperature: 300 °C as well as Gas: 99.99% He Temperature of Injector: 250 °C Range of Scan: m/z 25-1000 Type of Injection: Splitless Oven Program: 16°C Limit 1 to 60 °C for three minutes. Ascend two from (60 to 180) °C at 7 °C/min Elevation 3: (180 to 280) °C at 8°C/min 280°C ramp four hold for three minutes. Throughout the methyl transesterification process, MCM-41 transforms the components of sunflower oil that are produced into components of biodiesel. Linoleic acid and methyl ester ($C_{17}H_{34}O_2$, 25.93%) are the primary components of the biodiesel product, according to MCM-41.

The second largest component is the methyl ester of palmitate acid ($C_{18}H_{34}O_2$, 21.92%), followed by ($C_{19}H_{38}O_2$, 16.21%). The biodiesel samples were synthesized from sunflower oil using GCMS analysis. The computation results for the different FAME concentrations are displayed in **Table 5**.

Table 5: methyl esters' concentration has been identified by an analysis using GC-MS.

No.	R.T (min)	Area Percentage	Chemical Formula	FAME	M.W
1	16.662	2.01	$C_{17}H_{34}O_2$	C17:0	270
2	19.131	21.92	$C_{18}H_{34}O_2$	C18:1	282.5
3	21.691	25.93	$C_{17}H_{34}O_2$	C17:0	270
4	21.905	10.87	$C_{19}H_{36}O_2$	C19:1	296.5
5	22.065	16.21	$C_{19}H_{38}O_2$	C19:0	298.5
6	24.121 others	11.62 5.44	$C_{18}H_{34}O_2$	C18:1	282.5

7.2 Physical with Chemical Characteristics of Biodiesel

Characteristics for biodiesel generated from sunflower oil have been revealed by measuring its kinematic viscosity, flash point, specific gravity, calorific value, and acid number—all critical factors for evaluating fuel efficiency. These measures aim to assess the physical attributes and quality of the locally generated biodiesel and compare it with the global standard qualities of diesel production. **Table 6** provides an example of these characteristics, and the findings demonstrate the high level of convergence between fuel characteristics created in laboratories and fuels produced worldwide.

Table 6: Characteristics of biodiesel which produced from sunflower oil.

Properties	Units	Test method	Min. limit	Max. limit	biodiesel value obtained from the current study
Kinematic viscosity in 27 °C	mm^2/sec	STM D-6751[60]	1.9	6	4.879, ASTM D-7042
Specific gravity at 15°C	-	EN-BD: EN 14214[61]	0.86	0.9	0.90, ASTM D-7042
Flash point	°C	STM D-6751[60]	55	130	93, ASTM D-6450
Calorific value	(MJ/kg)	EN14213[62]	30	35	41.96, ASTM D-240
Acid value	Milligrams of KOH/gram of oil	STM D-6751[60]	0.5	1	0.5

8. Conclusion

The investigation concluded that the MCM-41 catalyst synthesized in a lab and prepared by the sol-gel method should be used to catalyse reactions, especially the transesterification of sunflower oil. After an hour, this yielded a 45%. Higher reaction temperatures, larger catalyst doses, and longer reaction periods were found to increase the yields of reaction products positively. The study also optimized the temperature, methanol/oil molar ratio, catalyst dose, and reaction time. A drop in catalytic efficiency was consequently brought on by extended reaction periods exceeding two hours. The results showed that (9:1) methanol/oil molar ratio and (1.25%) for catalyst dose at 60°C with an 800-rpm agitation speed would yield the maximum amount of biodiesel. The results show that the pure mesoporous MCM-41 silica is inactive due to its very weak acidity. The physical characteristics of biodiesel derived from sunflower oils were investigated as well as compared with the conventional fuel production processes. Comparative results confirmed that the biodiesel fuel generated was sufficient to be utilized as a substitute fuel source. Heterogeneous (solid catalyst) was successfully isolated from products, reactivated, and utilized in later procedures to create biodiesel with a good yield. As this study demonstrates, this helps lower the process's overall economic cost.

Acknowledgment
The authors thank the Department of Chemical Engineering, University of Technology–Iraq, Baghdad, Iraq for the support.

Conflict of Interest
The authors declare that they have no conflict of interest.

References
[1] F. Esmi, V. B. Borugadda, and A. K. Dalai, "Heteropoly acids as supported solid acid catalysts for sustainable biodiesel production using vegetable oils: A review," Catalysis Today, vol. 404, pp. 19-34, 2022/11/15/ 2022. doi:10.1016/j.cattod.2022.01.019.
[2] S. Khan, M. Naushad, J. Iqbal, C. Bathula, and G. Sharma, "Production and harvesting of microalgae and an efficient operational approach to biofuel production for a sustainable environment," Fuel, vol. 311, p. 122543, 2022/03/01/ 2022. doi:10.1016/j.fuel.2021.122543.
[3] M. H. Jayed, H. H. Masjuki, R. Saidur, M. A. Kalam, and M. I. Jahirul, "Environmental aspects and challenges of oilseed produced biodiesel in Southeast Asia," Renewable and Sustainable Energy Reviews, vol. 13, no. 9, pp. 2452-2462, 2009/12/01/ 2009. doi:10.1016/j.rser.2009.06.023.
[4] I. M. Rizwanul Fattah, M. A. Kalam, H. H. Masjuki, and A. Wakil, "Biodiesel production, characterization, engine performance, and emission characteristics of Malaysian Alexandrian laurel oil," RSC Advances, vol. 4, pp. 17787-17796, 04/10 2014.doi:10.1039/C3RA47954D.
[5] J. Najeeb et al., "Nanobiocatalysts for Biodiesel Synthesis through Transesterification—A Review," Catalysts, vol. 11, no. 2. doi: 10.3390/catal11020171 .
[6] F. Ma and M. A. Hanna, "Biodiesel production: a review Series #12109, Agricultural Research Division, Institute of Agriculture and Natural Resources, University of Nebraska–Lincoln.1," Bioresource Technology, vol. 70, no. 1, pp. 1-15, 1999/10/01/ 1999. doi:10.1016/j.apcato.2024.206999.
[7] T. Parangi and M. K. Mishra, "Solid Acid Catalysts for Biodiesel Production," Comments on Inorganic Chemistry, vol. 40, no. 4, pp. 176-216, 2020/07/03 2020. doi:10.1080/02603594.2020.1755273.
[8] S. H. Teo, A. Islam, and Y. H. Taufiq-Yap, "Algae derived biodiesel using nanocatalytic transesterification process," Chemical Engineering Research and Design, vol. 111, pp. 362-370, 2016/07/01/ 2016. doi:10.1016/j.cherd.2016.04.012.
[9] S. Alaei, M. Haghighi, J. Toghiani, and B. Rahmani Vahid, "Magnetic and reusable MgO/MgFe2O4 nanocatalyst for biodiesel production from sunflower oil: Influence of fuel ratio in combustion synthesis on catalytic properties and performance," Industrial Crops and Products, vol. 117, pp. 322-332, 2018/07/01/ 2018. doi:10.1016/j.indcrop.2018.03.015.
[10] K. Seffati, B. Honarvar, H. Esmaeili, and N. Esfandiari, "Enhanced biodiesel production from chicken fat using CaO/CuFe2O4 nanocatalyst and its combination with diesel to improve fuel properties," Fuel, vol. 235, pp. 1238-1244, 2019/01/01/ 2019. doi.:10.1016/j.fuel.2018.08.118.
[11] H. Rasouli and H. Esmaeili, "Characterization of MgO nanocatalyst to produce biodiesel from goat fat using transesterification process," 3 Biotech, vol. 9, no. 11, p. 429, 2019/10/30 2019. doi:10.1007/s13205-019-1963-6
[12] T. A. Degfie, T. T. Mamo, and Y. S. J. S. r. Mekonnen, "Optimized biodiesel production from waste cooking oil (WCO) using calcium oxide (CaO) nano-catalyst," vol. 9, no. 1, p. 18982, 2019. doi: 10.1038/s41598-019-55403-4.
[13] T. T. Mamo and Y. S. Mekonnen, "Microwave-Assisted Biodiesel Production from Microalgae, Scenedesmus Species, Using Goat Bone–Made Nano-catalyst," Applied Biochemistry and Biotechnology, vol. 190, no. 4, pp. 1147-1162, 2020/04/01 2020.doi: 10.1007/s12010-019-03149-0.
[14] A. Fallah Kelarijani, N. Gholipour Zanjani, and A. Kamran Pirzaman, "Ultrasonic Assisted Transesterification of Rapeseed Oil to Biodiesel Using Nano Magnetic Catalysts," Waste and Biomass Valorization, vol. 11, no. 6, pp. 2613-2621, 2020/06/01 2020. doi: 10.1007/s12649-019-00593-1.
[15] M. Hanif, I. A. Bhatti, K. Shahzad, and M. A. Hanif, "Biodiesel Production from Waste Plant Oil over a Novel Nano-Catalyst of Li-TiO2/Feldspar," Catalysts, vol. 13, no. 2. doi: 10.3390/catal13020310 .
[16] A. Satapathy, K. Saikia, and S. L. Rokhum, "Biodiesel Production Using a Banana Peel Extract-Mediated Highly Basic Heterogeneous Nanocatalyst," Sustainability, vol. 15, no. 14. doi: 10.3390/su151411332 .

[17] B. Hadi Jume et al., "Optimization of microreactor-assisted transesterification for biodiesel production using bimetal zirconium-titanium oxide doped magnetic graphene oxide heterogeneous nanocatalyst," Chemical Engineering and Processing - Process Intensification, vol. 191, p. 109479, 2023/09/01/ 2023. doi: 10.1016/j.psep.2023.03.039.

[18] S. Arshad et al., "Assessing the potential of green CdO2 nano-catalyst for the synthesis of biodiesel using non-edible seed oil of Malabar Ebony," Fuel, vol. 333, p. 126492, 2023/02/01/ 2023. doi: 10.1016/j.fuel.2022.126492

[19] J. V. L. Ruatpuia et al., "Microwave-assisted biodiesel production using ZIF-8 MOF-derived nanocatalyst: A process optimization, kinetics, thermodynamics and life cycle cost analysis," Energy Conversion and Management, vol. 292, p. 117418, 2023/09/15/ 2023. doi: 10.1016/j.enconman.2023.117418 .

[20] G. Farokhi, M. Saidi, and A. T. Najafabadi, "Application of spinel Type NixZn1−xFe2O4 magnetic nanocatalysts for biodiesel production from neem seed oil: Catalytic performance evaluation and optimization," Industrial Crops and Products, vol. 192, p. 116035, 2023/02/01/ 2023. doi: 10.1016/j.indcrop.2022.116035.

[21] S. Sahu, K. Saikia, B. Gurunathan, A. Dhakshinamoorthy, and S. L. Rokhum, "Green synthesis of CaO nanocatalyst using watermelon peels for biodiesel production," Molecular Catalysis, vol. 547, p. 113342, 2023/08/01/ 2023. doi: 10.1016/j.mcat.2023.113342.

[22] A. Aziz et al., "Novel Copper Oxide Phyto-Nanocatalyst Utilized for the Synthesis of Sustainable Biodiesel from Citrullus colocynthis Seed Oil," Processes, vol. 11, no. 6. doi: 10.3390/pr11061857.

[23] B. Maleki and H. Esmaeili, "Application of Fe3O4/SiO2@ZnO magnetic composites as a recyclable heterogeneous nanocatalyst for biodiesel production from waste cooking oil: Response surface methodology," Ceramics International, vol. 49, no. 7, pp. 11452-11463, 2023/04/01/ 2023. doi:10.1016/j.ceramint.2022.11.344

[24] M. T. Akhtar et al., "Sustainable Production of Biodiesel from Novel Non-Edible Oil Seeds (Descurainia sophia L.) via Green Nano CeO2 Catalyst," Energies, vol. 16, no. 3. doi: 10.3390/en16031534 .

[25] V. R. Kattimani, K. V. Yatish, K. Pramoda, M. Sakar, and R. G. Balakrishna, "Acacia furnesiana plant as a novel green source for the synthesis of NiFe2O4 magnetic nanocatalyst and as feedstock for sustainable high quality biofuel production," Fuel, vol. 348, p. 128549, 2023/09/15/ 2023. doi:10.1016/j.fuel.2023.128549.

[26] S. Echaroj, N. Pannucharoenwong, K. Duanguppama, P. Rattanadecho, and S. Hemathulin, "High throughput biodiesel production from waste cooking oil over metal oxide binded with Fe2O3," Energy Reports, vol. 9, pp. 205-215, 2023/09/01/ 2023. doi: 10.1016/j.egyr.2023.05.271.

[27] H. M. A. Hassan et al., "Biogenic-Mediated Synthesis of the Cs2O–MgO/MPC Nanocomposite for Biodiesel Production from Olive Oil," ACS Omega, vol. 5, no. 43, pp. 27811-27822, 2020/11/03 2020. doi: 10.1021/acsomega.0c02814.

[28] B. H. Jume, M. A. Gabris, H. Rashidi Nodeh, S. Rezania, and J. Cho, "Biodiesel production from waste cooking oil using a novel heterogeneous catalyst based on graphene oxide doped metal oxide nanoparticles," Renewable Energy, vol. 162, pp. 2182-2189, 2020/12/01/ 2020. doi:10.1016/j.renene.2020.10.046.

[29] Y. Wan, Y. Shi, and D. Zhao, "Supramolecular Aggregates as Templates: Ordered Mesoporous Polymers and Carbons," Chemistry of Materials, vol. 20, no. 3, pp. 932-945, 2008/02/01 2008. doi: 10.1021/cm7024125.

[30] I. K. Mbaraka and B. H. Shanks, "Conversion of oils and fats using advanced mesoporous heterogeneous catalysts," Journal of the American Oil Chemists' Society, vol. 83, no. 2, pp. 79-91, 2006/02/01 2006. doi: 10.1007/s11746-006-1179-x.

[31] H. Wu, J. Zhang, Y. Liu, J. Zheng, and Q. Wei, "Biodiesel production from Jatropha oil using mesoporous molecular sieves supporting K2SiO3 as catalysts for transesterification," Fuel Processing Technology, vol. 119, pp. 114-120, 2014/03/01/ 2014. doi: 10.1016/j.fuproc.2013.10.021.

[32] M. R. Mello, D. Phanon, G. Q. Silveira, P. L. Llewellyn, and C. M. Ronconi, "Amine-modified MCM-41 mesoporous silica for carbon dioxide capture," Microporous and Mesoporous Materials, vol. 143, no. 1, pp. 174-179, 2011/08/01/ 2011.doi: 10.1016/j.fuproc.2013.10.021.

[33] W. Xie and M. Fan, "Biodiesel production by transesterification using tetraalkylammonium hydroxides immobilized onto SBA-15 as a solid catalyst," Chemical Engineering Journal, vol. 239, pp. 60-67, 2014/03/01/ 2014. doi: 10.1016/j.cej.2013.11.009.

[34] P. K. Jal, S. Patel, and B. K. Mishra, "Chemical modification of silica surface by immobilization of functional groups for extractive concentration of metal ions," Talanta, vol. 62, no. 5, pp. 1005-1028, 2004/04/19/ 2004. doi: 10.1016/j.talanta.2003.10.028.

[35] J. Dias, M. Alvim-Ferraz, and M. Almeida, "Comparison of the performance of different homogeneous alkali catalysts during transesterification of waste and virgin oils and evaluation of biodiesel quality," Fuel, vol. 87, pp. 3572-3578, 12/01 2008. doi:10.1016/j.fuel.2008.06.014.

[36] A. P. Soares Dias, J. Puna, M. J. Neiva Correia, I. Nogueira, J. Gomes, and J. Bordado, "Effect of the oil acidity on the methanolysis performances of lime catalyst biodiesel from waste frying oils (WFO)," Fuel Processing Technology, vol. 116, pp. 94-100, 2013/12/01/ 2013. doi:10.1016/j.clet.2020.100012.

[37] S. M. Alardhi et al., "Investigating the capability of MCM-41 nanoparticle for COD removal from Iraqi petroleum refinery wastewater," in AIP Conference Proceedings, 2023, vol. 2820, no. 1: AIP Publishing. doi: 10.1063/5.0151096.

[38] N. A. Atiyah, T. M. Albayati, and M. A. Atiya, "Functionalization of mesoporous MCM-41 for the delivery of curcumin as an anti-inflammatory therapy," Advanced Powder Technology, vol. 33, no. 2, p. 103417, 2022. doi:10.1016/j.apt.2021.103417.

[39] A. Patel, N. J. C. S. Narkhede, and Technology, "Biodiesel synthesis via esterification and transesterification over a new heterogeneous catalyst comprising lacunary silicotungstate and MCM-41," vol. 3, no. 12, pp. 3317-3325, 2013. doi:10.1039/C3CY00591G.

[40] P. Muchan, C. Saiwan, and M. Nithitanakul, "Carbon dioxide adsorption/desorption performance of single- and blended-amines-impregnated MCM-41 mesoporous silica in post-combustion carbon capture," Clean Energy, vol. 6, pp. 424-437, 06/01 2022. doi: 10.1093/ce/zkac020.

[41] S. Garcés Polo, J. Villarroel-Rocha, K. Sapag, S. A. Korili, and A. Gil, "A comparative study of CO2 diffusion from adsorption kinetic measurements on microporous materials at low pressures and temperatures," Chemical Engineering Journal, vol. 302, 05/01 2016. doi: 10.1016/j.cej.2016.05.057.

[42] S. Alardhi, J. Alrubaye, and T. Albayati, "Adsorption of Methyl Green dye onto MCM-41: equilibrium, kinetics and thermodynamic studies," Desalination and Water Treatment, vol. 179, pp. 323–331, 02/25 2020. doi: 10.5004/dwt.2020.25000.

[43] J. A. Costa et al., "A new functionalized MCM-41 mesoporous material for use in environmental applications," vol. 25, pp. 197-207, 2014. doi: 10.5935/0103-5053.20130284.

[44] H. Chen, S. Fu, L. Fu, H. Yang, and D. Chen, "Simple Synthesis and Characterization of Hexagonal and Ordered Al–MCM–41 from Natural Perlite," Minerals, vol. 9, p. 264, 04/30 2019. doi: 10.3390/min9050264.

[45] N. Ali, N. Jabbar, S. Alardhi, H. Majdi, and T. Albayati, "Adsorption of methyl violet dye onto a prepared bio-adsorbent from date seeds: isotherm, kinetics, and thermodynamic studies," Heliyon, vol. 8, p. e10276, 08/01 2022. doi: 10.1016/j.heliyon.2022.e10276.

[46] M. Ebrahimi-Gatkash, H. Younesi, A. Shahbazi, and A. Heidari, "Amino-functionalized mesoporous MCM-41 silica as an efficient adsorbent for water treatment: batch and fixed-bed column adsorption of the nitrate anion," Applied Water Science, vol. 7, 11/18 2015. doi: 10.1007/s13201-015-0364-1.

[47] N. Vardast, M. Haghighi, and S. Dehghani, "Sono-dispersion of calcium over Al-MCM-41used as a nanocatalyst for biodiesel production from sunflower oil: Influence of ultrasound irradiation and calcium content on catalytic properties and performance," Renewable Energy, vol. 132, pp. 979-988, 2019/03/01/ 2019. doi: 10.1016/j.renene.2018.08.046.

[48] S. Dehghani and M. Haghighi, "Sono-dispersed MgO over cerium-doped MCM-41 nanocatalyst for biodiesel production from acidic sunflower oil: Surface evolution by altering Si/Ce molar ratios," Waste Management, vol. 95, pp. 584-592, 2019/07/15/ 2019. doi: 10.1016/j.wasman.2019.05.042.

[49] A. J. C. Steluti, O. C. da Motta Lima, and N. C. J. A. S. T. Pereira, "The influence of temperature on the rheology of biodiesel and on the biodiesel-glycerin-ethanol blend," vol. 34, no. 1, pp. 9-12, 2012. doi: 10.4025/actascitechnol.v34i1.8067.

[50] N. Supamathanon, "Biodiesel production via transesterification of jatropha seed oil using potassium supported on nay zeolite and mcm-41 as catalysts," School of Chemistry Institute of Science Suranaree University of technology, 2011. doi: 10.1016/j.enconman.2018.07.053.

[51] D. Kumar, G. Kumar, Poonam, and C. P. Singh, "Fast, easy ethanolysis of coconut oil for biodiesel production assisted by ultrasonication," Ultrasonics Sonochemistry, vol. 17, no. 3, pp. 555-559, 2010/03/01/ 2010. doi: 10.1016/j.ultsonch.2009.10.018.

[52] X. Yin, H. Ma, Q. You, Z. Wang, and J. Chang, "Comparison of four different enhancing methods for preparing biodiesel through transesterification of sunflower oil," Applied Energy, vol. 91, 03/01 2012. doi: 10.1016/j.apenergy.2011.09.016.

[53] A. Mohod, A. Subudhi, and P. Gogate, "Intensification of esterification of non edible oil as sustainable feedstock using cavitational reactors," Ultrasonics Sonochemistry, vol. 36, 12/01 2016. doi: 10.1016/j.ultsonch.2016.11.040.

[54] S. Mohan, A. Pal, and R. Singh, "The production of semal oil methyl esters through a combined process reactor," Energy Sources, Part A: Recovery, Utilization, and Environmental Effects, vol. 39, pp. 1-8, 04/12 2017. doi: 10.1080/15567036.2016.1235059.

[55] G. Lemoine, "Comparison of different types of zeolites used as solid acid catalysts in the transesterification reaction of Jatropha-type oil for biodiesel production," Worcester Polytechnic Institute, 2013.

[56] A. Sarve, M. Varma, and S. Sonawane, "Ultrasound Assisted Two-stage Biodiesel Synthesis from Non-edible Schleichera triguga oil using Heterogeneous catalyst: Kinetics and Thermodynamic analysis," Ultrasonics Sonochemistry, vol. 29, pp. 288-298, 09/01 2016. doi: 10.1016/j.ultsonch.2015.09.016.

[57] R. Jogi, M. Yedithasatyam, M. Rama Surya Satyanarayana, T. Rao, and J. Syed, "Biodiesel production from degummed Jatropha curcas oil using constant-temperature ultrasonic water bath," Energy Sources Part A Recovery Utilization and Environmental Effects, vol. 38, pp. 2610-2616, 09/01 2016. doi: 10.1016/j.cattod.2011.08.050

[58] A. Casas, C. M. Fernández, M. J. Ramos, Á. Pérez, and J. F. J. F. Rodríguez, "Optimization of the reaction parameters for fast pseudo single-phase transesterification of sunflower oil," vol. 89, no. 3, pp. 650-658, 2010. doi: 10.1016/j.fuel.2009.08.004.

[59] X. Deng, Z. Fang, Y.-h. Liu, and C.-L. J. E. Yu, "Production of biodiesel from Jatropha oil catalyzed by nanosized solid basic catalyst," vol. 36, no. 2, pp. 777-784, 2011. doi:10.1016/j.ultsonch.2013.10.023

[60] P. M. Medeiros, "Gas Chromatography–Mass Spectrometry (GC–MS)," in Encyclopedia of Geochemistry: A Comprehensive Reference Source on the Chemistry of the Earth, W. M. White, Ed. Cham: Springer International Publishing, 2018, pp. 530-535.

[61] C. J. W. C. ASTM, USA, "150: The American Society for Testing Materials Standard Specification for Portland Cement," 2002.

[62] M. Erdmann et al., "Photo-oxidation of PE-HD affecting polymer/fuel interaction and bacterial attachment," npj Materials Degradation, vol. 4, no. 1, p. 18, 2020/07/09 2020. doi: 10.1038/s41529-020-0122-1.